

# Three-dimensional MHD duct flows with strong transverse magnetic fields. Part 4. Fully insulated, variable-area rectangular ducts with small divergences

By J. S. WALKER

Department of Theoretical and Applied Mechanics, University of Illinois

AND G. S. S. LUDFORD

Department of Theoretical and Applied Mechanics, Cornell University

(Received 10 August 1972)

Part 3 of this study treats a prototype with insulating side walls at  $z = \pm 1$  for all  $x$  and insulating top and bottom walls at  $y = \pm a$  for  $x < 0$  and at  $y = \pm (a + bx)$  for  $x > 0$ , where the applied magnetic field is in the  $y$  direction and the flow is in the  $x$  direction. In the diverging portion ( $x > 0$ ) of this duct, the entire mass flux is carried by high-velocity jets adjacent to the side walls, while the fluid elsewhere is stagnant. In the constant-area portion ( $x < 0$ ), the fully developed flow is severely disturbed as it approaches the join at  $x = 0$ , and high-velocity jets occur even before the top and bottom walls begin to diverge. The analysis presented in Part 3 is not valid in the limit  $b \rightarrow 0$ , and the object of this paper is to reconcile the stagnant core flow for  $b \neq 0$  with the fully developed flow for  $b = 0$ . Conditions are such that inertia forces are negligible.

The first transitional stage occurs when  $1 \gg b \gg M^{-\frac{1}{2}}$ , where  $M$  is the (large) Hartmann number. The upstream disturbance disappears, and downstream each of the  $O(M^{-\frac{1}{2}})$  side-wall boundary layers splits into an  $O(b^{-1}M^{-\frac{1}{2}})$  outer layer and an  $O(M^{-\frac{1}{2}})$  inner layer. The fluid outside these layers is still stagnant and an  $O(bM^{\frac{1}{2}})$  velocity in the outer sublayers accounts for the mass flux. The viscous inner sublayers reduce the velocity in the outer sublayers to zero at the side walls.

The second transitional stage occurs when  $b = O(M^{-\frac{1}{2}})$ . The outer sublayers spread across the entire duct so that none of the fluid is stagnant, and an  $O(1)$  core velocity accounts for the mass flux. This analysis is valid no matter how small  $b$  becomes, and as  $b \rightarrow 0$  the fully developed solution is recovered everywhere.

---

## 1. Introduction

In Part 3, Walker, Ludford & Hunt (1972) analysed the flow in a prototype variable-area rectangular duct with insulating walls and developed a procedure for extending this analysis to general fully insulated ducts. This prototype has parallel side walls at  $z = \pm 1$  for all  $x$  and top and bottom walls at  $y = \pm a$  for  $x < 0$  and at  $y = \pm (a + bx)$  for  $x > 0$ , where the applied magnetic field is in the

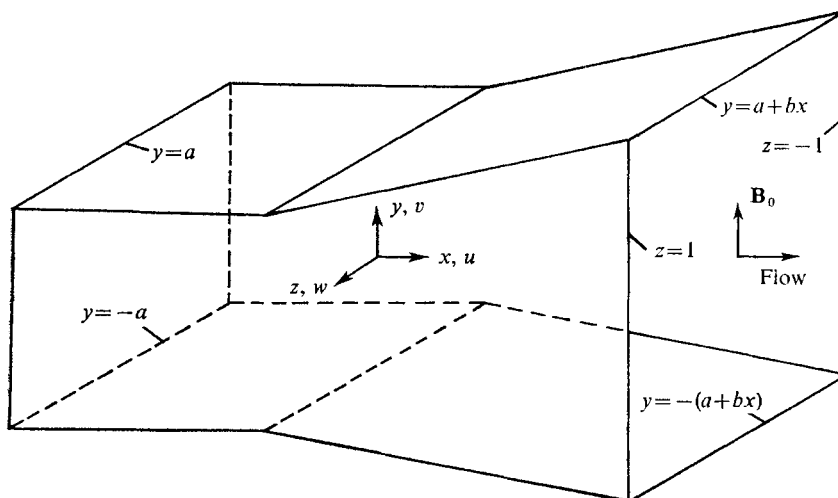


FIGURE 1. Duct with insulating walls.

$y$  direction and the centre-line of the duct is taken as the  $x$  axis (see figure 1). For  $x > 0$ , high-velocity jets within thin boundary layers adjacent to the side walls account for the entire mass flux. The fluid outside of these layers is stagnant because the electric current for the Lorentz force needed to drive it across the strong magnetic field is blocked by the insulating side walls. The high-velocity jets are held against the side walls by Lorentz forces which are produced by electric currents flowing in the  $\pm x$  direction within the side layers at  $z = \pm 1$ . At the join ( $x = 0$ ), these current lines continue back into the side layers in the constant-area portion ( $x < 0$ ) and remain within these layers sufficiently far upstream for the current flux to be redistributed in the  $y$  direction. The electrical circuit is closed by a plane potential current flow (which is uniform in the  $y$  direction) across the constant-area portion of the duct. As  $x \rightarrow -\infty$ , the high-velocity side layers disappear and the fully developed flow in a constant-area insulated rectangular duct is recovered (Shercliff 1953; Roberts 1967), with the non-dimensional velocity equal to one everywhere except near the walls. It is the currents in the side layers near  $x = 0$  which produce the Lorentz forces drawing fluid into these layers. In other words, the fully developed flow approaching the join is severely disturbed and high-velocity jets adjacent to the side walls occur even before the divergence begins at  $x = 0$ . A free shear layer across the section  $x = 0$  absorbs whatever mass flux has not been drawn into the side layers upstream and delivers half of it to each of the downstream side layers, so that each carries half of the total flux. Some streamlines and current lines in a  $y$  section of the duct are sketched in figure 2(a). The fraction of the total flux carried by the upstream side layers as they enter  $x = 0^-$  reflects the severity of the disturbance in the constant-area portion; it tends to zero as  $b$  approaches zero, though the analysis presented in Part 3 is not valid in this limit.

For  $b = 0$ , we have a constant-area duct for all  $x$  and there is fully developed flow everywhere. To complete the study of fully insulated variable-area rectangular ducts, we must show how the solution presented in Part 3, with

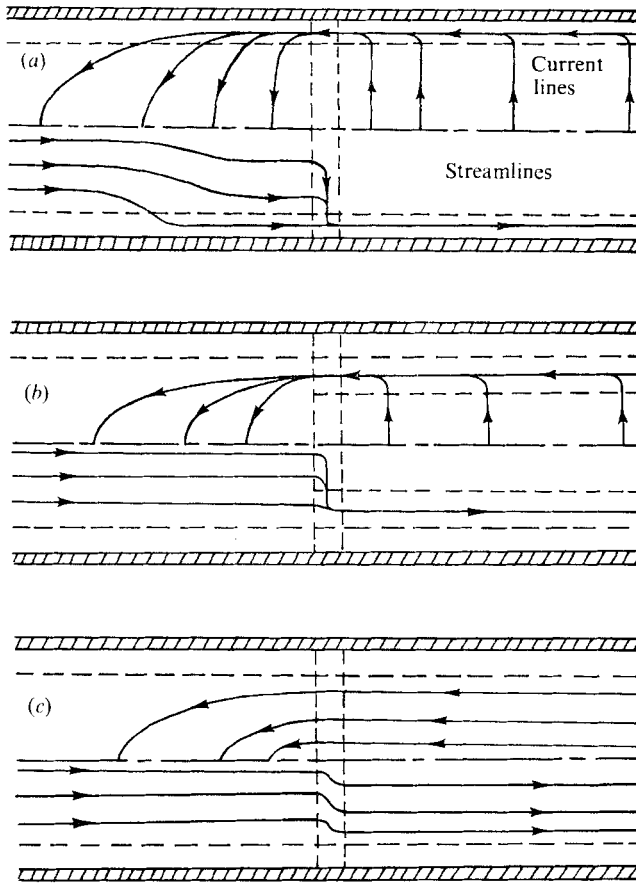


FIGURE 2.  $y$  sections showing current lines and streamlines for (a)  $b = O(1)$ , (b)  $1 \gg b \gg M^{-1/2}$  and (c)  $b = O(M^{-1/2})$ .

its high-velocity side layers, evolves into the radically different fully developed solution as  $b \rightarrow 0$ . First we shall treat the two transitional stages involved between  $b = O(1)$  and  $b = 0$ , namely  $1 \gg b \gg M^{-1/2}$  and  $b = O(M^{-1/2})$ , where  $M$  is the Hartmann number. Then we shall extend these two solutions to general, slowly varying, fully insulated, rectangular ducts.

In the first transitional stage  $1 \gg b \gg M^{-1/2}$  (see § 3), the upstream high-velocity jets disappear and the fully developed flow in the constant-area portion ( $x < 0$ ) remains undisturbed until it enters the free shear layer at the join. Each of the downstream side layers splits into an inner and an outer sublayer. Half the total mass flux is now carried by each of the outer sublayers, whose thickness has grown by a factor  $b^{-1}$ , so that the velocity needed to carry the mass flux has decreased by a factor  $b$ . The viscous inner sublayer lies between the outer sublayer and the side wall, reducing the velocity in the former to zero at the latter. The high-velocity jets are still held against the side walls by Lorentz forces produced by electric currents flowing along the duct within the outer sublayers, but now these currents are uniform in the  $y$  direction. Upstream, the electrical

circuit is closed by a plane potential current flow from a current source at  $x = 0$ ,  $z = -1$  to a current sink at  $x = 0$ ,  $z = +1$ . The role of the free shear layer remains essentially the same. Several streamlines and current lines in a  $y$  section of this duct are sketched in figure 2(b).

In the second transitional stage  $b = O(M^{-\frac{1}{2}})$  (see § 4), the outer sublayers have spread across the entire diverging portion of the duct, so that none of the fluid is stagnant and the mass flux is carried by  $O(1)$  velocities everywhere. The flow in the diverging portion is not constant with  $z$ , the variations being maintained by currents flowing in the positive- $x$  direction for  $z > 0$  and in the negative- $x$  direction for  $z < 0$ . The electrical circuit is once again closed in the constant-area portion by a plane potential current flow, but now current flows out of the free shear layer everywhere for  $z < 0$  and into it everywhere for  $z > 0$ . Figure 2(c) shows a sketch of several streamlines and current lines in a  $y$  section of this duct. The analysis for this transitional stage is valid no matter how small  $b$  becomes. As  $b \rightarrow 0$ , the downstream flow becomes constant with  $z$  (as well as  $x$  and  $y$ ), the  $x, z$  circulation of current disappears and fully developed flow is recovered everywhere.

In Part 3 the extension of the analysis for the prototype to a rectangular duct with insulating walls at  $z = \pm 1$  and  $y = \pm f(x)$  involves an elaborate numerical procedure which ignores the effects of wall curvature. When  $|f'(x)| \ll 1$ , the flow is locally identical to that in the prototype with  $b = f'(x)$ , and the analysis presented here in §§ 3 and 4 is easily extended to general, slowly varying, fully insulated, rectangular ducts (§ 5). The solutions are initially given for the prototype rather than for the general duct in order to illustrate the basic phenomena in the simplest possible context and to provide a direct comparison with the results of Part 3.

## 2. General considerations

If the induced magnetic field and the fluid inertia are negligible, the non-dimensional equations governing the steady flow of an electrically conducting liquid of uniform properties under the action of a transverse magnetic field  $\mathbf{B}_0 = B_0 \hat{\mathbf{y}}$  are

$$\partial^2 \phi / \partial y^2 = M^{-2} \nabla^4 \phi, \quad \partial v / \partial y = \nabla^2 h, \quad \partial h / \partial y = M^{-2} \nabla^2 v, \quad (1a, b, c)$$

$$u = -\partial \phi / \partial z - \partial h / \partial x + M^{-2} \nabla^2 u, \quad w = \partial \phi / \partial x - \partial h / \partial z + M^{-2} \nabla^2 w, \quad (1d, e)$$

$$j_x = \partial h / \partial z - M^{-2} \nabla^2 w, \quad j_y = \partial \phi / \partial y, \quad j_z = -\partial h / \partial x + M^{-2} \nabla^2 u \quad (1f, g, h)$$

(see Part 3). Here  $u, v$  and  $w$  are the components of the fluid velocity (see figure 1),  $j_x, j_y$  and  $j_z$  are the components of the electric current density,  $\phi$  is the electric potential,  $h$  is the pressure (referred to the characteristic Lorentz force per unit area  $\sigma U_0 B_0^2 d$ ) and

$$M = B_0 d (\sigma / \eta)^{\frac{1}{2}}$$

is the Hartmann number. Half the distance between the parallel side walls of our prototypic duct has been used as the characteristic length  $d$  and the average

velocity at some upstream section ( $x < 0$ ) has been used as the characteristic velocity  $U_0$ . Thus

$$\int_{-1}^1 \int_{-f(x)}^{f(x)} u(x, y, z) dy dz = 4a, \quad \text{where } f(x) = \begin{cases} a & \text{for } x < 0, \\ a + bx & \text{for } x > 0. \end{cases} \quad (2)$$

The boundary conditions

$$\mathbf{v} = 0, \quad j_y = \pm f'(x) j_x \quad \text{at } y = \pm f(x), \quad (3a)$$

$$\mathbf{v} = 0, \quad j_z = 0 \quad \text{at } z = \pm 1, \quad (3b)$$

and the governing equations (1) form a homogeneous problem whose solution is normalized by the mass-flux condition (2).

The Hartmann number is the only parameter in this boundary-value problem and under the assumption that  $M \gg 1$  the flow region may be divided into a central core in the constant-area portion of the duct ( $x < 0$ ), another core in the diverging portion ( $x > 0$ ), a free shear layer across the join ( $x = 0$ ) and thin boundary layers in the fluid adjacent to the duct walls. The boundary layers at  $y = \pm f(x)$  are the well-known Hartmann layers, which have a locally determined exponential structure matching the core variables provided that the latter satisfy the Hartmann conditions

$$v \mp f' u = O(M^{-1}),$$

$$j_y \mp f' j_x = \pm M^{-1}(\partial w / \partial x - \partial u / \partial z) + M^{-1} f' (\partial w / \partial y - \partial v / \partial z) + O(M^{-2})$$

at  $y = \pm f(x)$  (see Part 3).

In Part 3, the key variables in every subregion of the flow were the  $O(1)$  electric potential and the  $O(M^{-\frac{1}{2}})$  pressure, and each of these served as a special type of stream function for the  $O(1)$  mass flux and the  $O(M^{-\frac{1}{2}})$  electric current flux respectively. Thus the jump in  $\phi$  across the side layer at  $z = -1$  at some  $y$  level and some  $x$  section was equal to the mass flux being carried by the layer at that level,

$$\Delta\phi = \int_0^\infty u(x, y, \zeta) d\zeta, \quad \zeta = M^{\frac{1}{2}}(z + 1).$$

For small values of  $b$ , these two variables play the same fundamental roles, namely, giving the leading terms in the expansions for  $\phi$  and  $h$  for both transitional stages. The order of magnitude of any other variable in any subregion of the flow will be determined from the order of magnitude of the derivatives in this subregion and the relationship given by the governing equations (1) between the variable and the key functions  $\phi$  and  $h$ .

### 3. Intermediate slope: $1 \gg b \gg M^{-\frac{1}{2}}$

When  $b$  is much less than one but much greater than  $M^{-\frac{1}{2}}$ , the appropriate small parameters to be taken as independent are  $b^{-1}M^{-\frac{1}{2}}$  and  $b$ . The various flow subregions for this transitional stage are shown in figure 3 and the orders of magnitude of the  $x$  and  $z$  derivatives in each subregion are given in table 1. Note that each of these subregions is separated from the top and bottom walls by

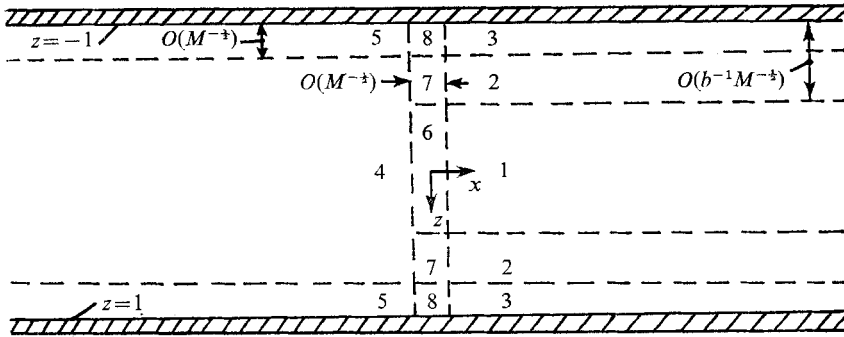


FIGURE 3. *y* section showing subregions for  $1 \gg b \gg M^{-\frac{1}{2}}$ .

Subregion	$\partial/\partial x$	$\partial/\partial z$
(1) Downstream core	$b$	$1$
(2) Downstream outer sublayer	$b$	$bM^{\frac{1}{2}}$
(3) Downstream inner sublayer	$b$	$M^{\frac{1}{2}}$
(4) Upstream core	$1$	$1$
(5) Upstream side layer	$1$	$M^{\frac{1}{2}}$
(6) Free shear layer	$M^{\frac{1}{2}}$	$1$
(7) Outer intersection	$M^{\frac{1}{2}}$	$bM^{\frac{1}{2}}$
(8) Inner intersection	$M^{\frac{1}{2}}$	$M^{\frac{1}{2}}$

TABLE 1. Order of magnitude of *x* and *z* derivatives in each subregion of the flow for an intermediate slope

Hartmann layers of thickness of  $O(M^{-1})$  and that these layers will be taken care of by applying Hartmann conditions at  $y = \pm f(x)$  to the variables in each subregion. We write  $\phi$  and  $h$  as double expansions in the two small parameters where the leading terms are of  $O(1)$  and  $O(M^{-\frac{1}{2}})$  respectively:

$$\begin{aligned} \phi &= \phi^{(0,0)} + b^{-1}M^{-\frac{1}{2}}\phi^{(0,1)} + b^{-2}M^{-1}\phi^{(0,2)} + \dots \\ &\quad + b\phi^{(1,0)} + M^{-\frac{1}{2}}\phi^{(1,1)} + b^{-1}M^{-1}\phi^{(1,2)} + \dots \\ &\quad + b^2\phi^{(2,0)} + bM^{-\frac{1}{2}}\phi^{(2,1)} + M^{-1}\phi^{(2,2)} + \dots, \\ h &= M^{-\frac{1}{2}}h^{(1,1)} + b^{-1}M^{-1}h^{(1,2)} + \dots \\ &\quad + bM^{-\frac{1}{2}}h^{(2,1)} + M^{-1}h^{(2,2)} + \dots \end{aligned}$$

Note that, as  $b$  approaches one, all the terms in a given column in either expansion sum to give a single term in the one-parameter expansions which were used in Part 3. The other variables may be much larger than one in subregions with large derivatives so we must use expansions such as

$$\begin{aligned} w &= M^{\frac{1}{2}}w^{(-1,-1)} + b^{-1}w^{(-1,0)} + b^{-2}M^{-\frac{1}{2}}w^{(-1,1)} + \dots \\ &\quad + bM^{\frac{1}{2}}w^{(0,-1)} + w^{(0,0)} + b^{-1}M^{-\frac{1}{2}}w^{(0,1)} + \dots \\ &\quad + b^2M^{\frac{1}{2}}w^{(1,-1)} + bw^{(1,0)} + M^{-\frac{1}{2}}w^{(1,1)} + \dots \end{aligned}$$

In the downstream core 1, the substitution  $X = bx$  compresses the  $x$  co-ordinate so that all derivatives are  $O(1)$ . On satisfying equations (1), the leading terms in the core expansions are found to be given by

$$\begin{aligned} \phi_1^{(0,0)} &= y\Omega + \Psi, & u_1^{(0,0)} &= -y(\partial\Omega/\partial z) - \partial\Psi/\partial z, \\ v_1^{(0,0)} &= G, & w_1^{(1,0)} &= y\partial\Omega/\partial X + \partial\Psi/\partial X, & h_1^{(1,1)} &= H, \\ j_{x1}^{(1,1)} &= \partial H/\partial z, & j_{y1}^{(0,0)} &= \Omega, & j_{z1}^{(2,1)} &= -\partial H/\partial X, \end{aligned}$$

where  $\Omega, \Psi, G$  and  $H$  are integration functions of  $X$  and  $z$ . We shall also need two higher order terms, which are given by

$$v_1^{(1,0)} = \hat{G}, \quad j_{y1}^{(2,1)} = \hat{\Omega}$$

in terms of two more integration functions of  $X$  and  $z$ . The Hartmann conditions which these variables must satisfy are

$$v_1^{(0,0)} = v_1^{(1,0)} \mp u_1^{(0,0)} = j_{y1}^{(0,0)} = j_{y1}^{(2,1)} \mp j_{x1}^{(1,1)} = 0 \quad \text{at } y = \pm(a + X),$$

and these conditions are simply that  $\Omega, G, \hat{\Omega}$  and  $\hat{G}$  are zero while  $\Psi$  and  $H$  are functions of  $X$  only. Thus the  $O(1)$  velocities vanish and as far as the  $O(1)$  mass flux is concerned, the core is stagnant. The minimum dissipation theorem implies that  $\Psi$  is also zero, so that the only non-zero core variables are

$$h_1^{(1,1)}(X) \quad \text{and} \quad j_{z1}^{(2,1)} = -dh_1^{(1,1)}/dX,$$

which will be determined by matching with the outer sublayer.

Since the flow is symmetric in  $z$ , we need only consider the downstream outer sublayer 2 at  $z = -1$ , where we use  $\xi = bM^{1/2}(z + 1)$  to stretch the local  $z$  co-ordinate and  $X = bx$  to compress the  $x$  co-ordinate. On satisfying equations (1), the leading terms are given by

$$\begin{aligned} \phi_2^{(0,0)} &= y\Omega + \Psi, & u_2^{(0,-1)} &= -y\partial\Omega/\partial\xi - \partial\Psi/\partial\xi, \\ v_2^{(1,-1)} &= y\partial^2 H/\partial\xi^2 + G, & w_2^{(1,0)} &= y\partial\Omega/\partial X + \partial\Psi/\partial X - \partial H/\partial\xi, \\ h_2^{(1,1)} &= H, & j_{x2}^{(1,0)} &= \partial H/\partial\xi, & j_{y2}^{(0,0)} &= \Omega, & j_{z2}^{(2,1)} &= -\partial H/\partial X, \end{aligned}$$

where  $\Omega, \Psi, H$  and  $G$  are unknown integration functions of  $X$  and  $\xi$  in the outer sublayer. We shall also need the  $y$  component of the  $O(b^2)$  current:  $j_{y2}^{(2,0)} = \hat{\Omega}(X, \xi)$ . In order to satisfy the Hartmann boundary conditions,

$$v_2^{(1,-1)} \mp u_2^{(0,-1)} = j_{y2}^{(0,0)} = j_{y2}^{(2,0)} \mp j_{x2}^{(1,0)} \pm \partial u_2^{(0,-1)}/\partial\xi = 0 \quad \text{at } y = \pm(a + X),$$

so  $\Omega, G$  and  $\hat{\Omega}$  must be zero, while  $\Psi$  and  $H$  must satisfy

$$\partial^2\Psi/\partial\xi^2 + \partial H/\partial\xi = (a + X)\partial^2 H/\partial\xi^2 + \partial\Psi/\partial\xi = 0.$$

The solution which matches the core solution as  $\xi \rightarrow \infty$  is

$$\Psi = \mathcal{F} \exp[-\xi(a + X)^{-1/2}], \quad H = h_1^{(1,1)} + \mathcal{F}(a + X)^{-1/2} \exp[-\xi(a + X)^{-1/2}],$$

where  $\mathcal{F}(X)$  and  $h_1^{(1,1)}(X)$  will be determined by matching with the inner sublayer.

The viscous inner sublayer 3 at  $z = -1$  satisfies the no-slip boundary condition at the wall and matches the outer sublayer. Since this sublayer does not carry

any  $O(1)$  mass flux or  $O(M^{-\frac{1}{2}})$  current flux, there are no variations in the  $O(1)$  electric potential or  $O(M^{-\frac{1}{2}})$  pressure across it. Thus we have

$$\phi_3^{(0,0)} = \mathcal{F}, \quad h_3^{(1,1)} = h_1^{(1,1)} + \mathcal{F}(a + X)^{-\frac{1}{2}}$$

throughout the inner sublayer. When the local  $z$  co-ordinate is stretched by introducing  $\zeta = M^{\frac{1}{2}}(z + 1) = b^{-1}\xi$ , the governing equations (1) together with the matching yield several additional simple results:

$$h_3^{(2,1)} = h_2^{(2,1)}(X, y, 0) - \zeta \mathcal{F}(a + X)^{-1}, \tag{4a}$$

$$w_3^{(1,0)} = d\mathcal{F}/dX + \mathcal{F}(a + X)^{-1}, \quad j_{z3}^{(1,0)} = -\mathcal{F}(a + X)^{-1}. \tag{4b, c}$$

Since  $w_3^{(1,0)}$  must be zero at the side wall, (4b) determines  $\mathcal{F}$  to within an integration constant,

$$\mathcal{F} = c(a + X)^{-1},$$

so that the  $x$  velocity in the outer sublayer is given by

$$u_2^{(0,-1)} = c(a + X)^{-\frac{3}{2}} \exp[-\xi(a + X)^{-\frac{1}{2}}].$$

Since this sublayer carries half the total mass flux, the flux condition (2) determines  $c$ :

$$\int_0^\infty \int_{-(a+X)}^{a+X} u_2^{(0,-1)} dy d\xi = 2c,$$

so that  $c = a$ .

The boundary-value problem governing  $\phi_3^{(1,0)}$  is decoupled from the one governing  $v_3^{(1,-1)}$  and  $h_3^{(3,1)}$ . As we shall see, the former determines the core pressure  $h_1^{(1,1)}$ , while the latter does not affect the solution in the other subregions and will not be treated here. Equation (1a) becomes

$$\partial^2 \phi_3^{(1,0)} / \partial y^2 = \partial^4 \phi_3^{(1,0)} / \partial \zeta^4 \tag{5a}$$

and the side-wall boundary conditions (3b) become

$$\partial \phi_3^{(1,0)} / \partial \zeta = 0, \quad \partial^3 \phi_3^{(1,0)} / \partial \zeta^3 = -dh_3^{(1,1)} / dX \quad \text{at} \quad \zeta = 0. \tag{5b}$$

The Hartmann conditions are

$$\partial \phi_3^{(1,0)} / \partial y \mp \partial^2 \phi_3^{(1,0)} / \partial \zeta^2 = 0 \quad \text{at} \quad y = \pm(a + X), \tag{5c}$$

while matching with the outer sublayer gives

$$\phi_3^{(1,0)} = \phi_2^{(1,0)}(X, y, 0) - a\zeta(a + X)^{-\frac{3}{2}} \quad \text{as} \quad \zeta \rightarrow \infty. \tag{5d}$$

In order to match the inner and outer sublayers, we set  $\xi = b\zeta$  in a given outer-sublayer expansion, expand each term as a power series in  $b$ , regroup terms to form a new double expansion whose coefficient functions are independent of  $b$  and  $M$ , and equate the resulting expansion term by term to the corresponding inner-sublayer expansion in the limit  $\zeta \rightarrow \infty$ . The unknown functions  $h_2^{(2,1)}(X, y, 0)$  and  $\phi_2^{(1,0)}(X, y, 0)$  appear in the solutions for  $h_3^{(2,1)}$  and  $\phi_3^{(1,0)}$  respectively. These higher order terms could easily be determined by extending this analysis beyond the leading term in each expansion. This extension is not given here because these functions are merely integration functions of  $X$  and  $y$  which play no significant role in our first-order solution.



In order to determine  $h_1^{(1,1)}$  we integrate (5a) over the semi-infinite strip  $|y| \leq a + X$ ,  $0 \leq \zeta < \infty$ , insist that the velocity  $u_3^{(0,-1)}$  be continuous at the corners, and introduce conditions (5b, c, d) to obtain

$$dh_1^{(1,1)}/dX = \frac{1}{2}a(a + X)^{-\frac{1}{2}}.$$

Therefore the  $O(M^{-\frac{1}{2}})$  pressure and  $O(bM^{-\frac{1}{2}})$  transverse current in the downstream core are given by

$$h_1^{(1,1)} = h_0 - \frac{1}{3}a(a + X)^{-\frac{1}{2}}, \quad j_{z1}^{(2,1)} = -\frac{1}{2}a(a + X)^{-\frac{1}{2}},$$

where  $h_0$  is a constant reference pressure which will be determined by matching the upstream core solution.

The functions  $H$  and  $\Psi$  having been determined, the outer sublayer variables are now given by

$$\begin{aligned} \phi_2^{(0,0)} &= a(a + X)^{-1} \exp[-\xi(a + X)^{-\frac{1}{2}}], \quad u_2^{(0,-1)} = -\partial\phi_2^{(0,0)}/\partial\xi, \\ h_2^{(1,1)} &= h_0 - a(a + X)^{-\frac{1}{2}}\{\frac{1}{3} - \exp[-\xi(a + X)^{-\frac{1}{2}}]\}, \\ v_2^{(1,-1)} &= y\partial^2h_2^{(1,1)}/\partial\xi^2, \quad w_2^{(1,0)} = \frac{1}{2}a\xi(a + X)^{-\frac{1}{2}} \exp[-\xi(a + X)^{-\frac{1}{2}}], \\ j_{x2}^{(1,0)} &= \partial h_2^{(1,1)}/\partial\xi, \quad j_{y2}^{(0,0)} = j_{z2}^{(0,0)} = 0, \quad j_{z2}^{(2,1)} = -\partial h_2^{(1,1)}/\partial X. \end{aligned}$$

In the inner sublayer, we now have

$$\phi_3^{(0,0)} = a(a + X)^{-1}, \quad h_3^{(1,1)} = h_0 + \frac{2}{3}a(a + X)^{-\frac{1}{2}},$$

and the boundary-value problem (5) governing  $\phi_3^{(1,0)}$ . By combining solutions of the forward and backward heat equation, we obtain

$$\phi_3^{(1,0)} + \phi_3^{(1,0)}(X, y, 0) + a(a + X)^{-\frac{1}{2}}[\phi^*(+y) + \phi^*(-y) - \zeta(a + X)],$$

where

$$\begin{aligned} \phi^*(X, y, \zeta) &= \frac{1}{2}\zeta[\frac{1}{8}\zeta^2 + a + X + y] \operatorname{erfc}[\frac{1}{2}\zeta(a + X + y)^{-\frac{1}{2}}] - \frac{2}{3}\pi^{-\frac{1}{2}} \\ &\quad \times (a + X + y)^{\frac{1}{2}}[\frac{1}{4}\zeta^2 + a + X + y] \exp[-\frac{1}{4}\zeta^2(a + X + y)^{-1}]. \end{aligned}$$

The related variables are given by equations (1d, g, h):

$$u_3^{(0,-1)} = -\frac{\partial\phi_3^{(1,0)}}{\partial\xi}, \quad j_{y3}^{(1,0)} = \frac{\partial\phi_3^{(1,0)}}{\partial y}, \quad j_{z3}^{(2,1)} = a(a + X)^{-\frac{1}{2}} - \frac{\partial^3\phi_3^{(1,0)}}{\partial\xi^3}.$$

This is essentially the boundary-layer solution for fully developed flow in a constant-area duct with the appropriate local scaling.

Half of the total  $O(1)$  mass flux is carried by the  $O(bM^{\frac{1}{2}})$  velocity  $u_2^{(0,-1)}$  in the outer sublayer. This high-velocity jet is held against the side wall by a Lorentz force produced by an  $O(M^{-\frac{1}{2}})$  current flux in the negative  $x$  direction through the outer sublayer. This current flux is maintained by the  $O(b)$  current  $j_{x2}^{(1,0)}$ , which is constant in the  $y$  direction. As  $X$  increases, the high-velocity layer spreads out in both the  $y$  and the  $\xi$  directions, so that less current is needed to hold it against the wall, the surplus flowing across the core as  $j_{z1}^{(2,1)}$ . Since  $j_{x2}^{(1,0)}$  is constant in  $y$ , part of the current flux is lost into the Hartmann layers at each cross-section. This current flows into the Hartmann layers adjacent to the inner sublayer and then into the inner layer itself, where it is turned and fed back into the outer sublayer.

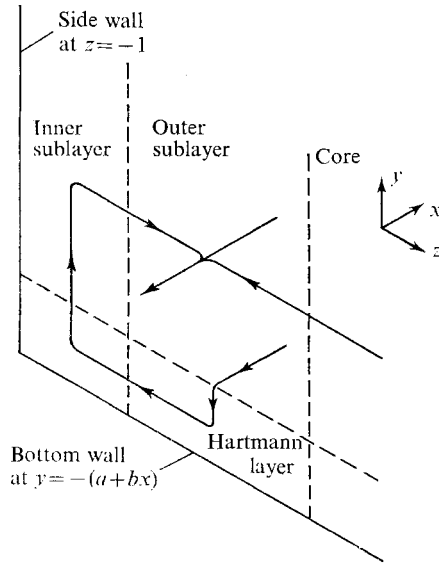


FIGURE 4. Downstream current paths for  $1 \gg b \gg M^{-\frac{1}{2}}$ .

A sketch of these current paths is shown in figure 4. Note that over an  $O(b^{-1})$  length of the duct, these currents represent a circulation of  $O(M^{-\frac{1}{2}})$  current flux.

In the constant-area portion of the duct ( $x < 0$ ), the disturbance due to the divergence downstream is of  $O(M^{-\frac{1}{2}})$ , the  $O(1)$  variables being given by the fully developed solution. All  $O(1)$  variables are zero except  $\phi^{(0,0)}$  and  $u^{(0,0)}$ , which are given by

$$\phi_4^{(0,0)} = -z, \quad u_4^{(0,0)} = 1$$

in the upstream core 4. Since the flow is symmetric in  $z$ , we need only consider the upstream side layer 5 at  $z = -1$ ; there the  $O(1)$  variables are

$$\phi_5^{(0,0)} = 1, \quad u_5^{(0,0)} = 1 - \frac{\partial \phi^*}{\partial \zeta}(0, +y, \zeta) - \frac{\partial \phi^*}{\partial \zeta}(0, -y, \zeta).$$

The profile function  $\phi^*(X, y, \zeta)$  and the co-ordinate  $\zeta$  are the same as for the downstream inner sublayer 3.

The flow in the free shear layer 6 is determined independently at each  $z$  section by the local electric potential jump across the layer. Its structure is given by

$$\phi_6^{(0,0)} = -\frac{1}{4}z[\hat{\phi}(\hat{x}, y) + \hat{\phi}(\hat{x}, -y)],$$

where

$$\hat{\phi} = \operatorname{erfc}(\frac{1}{2}\hat{x}(a+y)^{-\frac{1}{2}}), \quad \hat{x} = M^{\frac{1}{2}}x$$

(see Part 3). The related variables are

$$u_6^{(0,0)} = -\partial \phi_6^{(0,0)} / \partial z, \quad w_6^{(-1,-1)} = \partial \phi_6^{(0,0)} / \partial \hat{x},$$

$$j_{x_6}^{(1,1)} = -\partial^3 \phi_6^{(0,0)} / \partial \hat{x}^3, \quad j_{y_6}^{(0,0)} = \partial \phi_6^{(0,0)} / \partial y.$$

There is no variation in the  $O(M^{-\frac{1}{2}})$  pressure across a free shear layer, so that

$$h_6^{(1,1)} = h_0 - \frac{1}{3}a^{-\frac{1}{2}}, \quad v_6^{(-1,-1)} = j_{z_6}^{(0,0)} = 0.$$

The  $O(1)$  mass flux, carried by  $u_4^{(0,0)}$  in the upstream core, passes into the free shear layer, where it is divided in half and turned towards the side walls. Each of these jets, involving an  $O(M^{\frac{1}{2}})$  transverse velocity, is carrying half of the total mass flux as it enters one of the outer intersections 7. Since  $j_{z6}^{(0,0)}$  is zero, the free layer does not channel any  $O(M^{-\frac{1}{2}})$  current flux across the duct.

In the outer intersection 7 at  $z = -1$ , the  $x$  co-ordinate is stretched by  $\hat{x} = M^{\frac{1}{2}}x$  and the  $z$  co-ordinate is stretched by  $\xi = bM^{\frac{1}{2}}(z + 1)$ . The solution is determined independently at each  $\xi$  section by the local electric potential jump, so that

$$\phi_7^{(0,0)} = \exp(-\xi a^{-\frac{1}{2}}) + \frac{1}{4}[1 - \exp(-\xi a^{-\frac{1}{2}})][\hat{\phi}(\hat{x}, y) + \hat{\phi}(\hat{x}, -y)],$$

and the related variables are

$$u_7^{(0,-1)} = -\partial\phi_7^{(0,0)}/\partial\xi, \quad w_7^{(-1,-1)} = \partial\phi_7^{(0,0)}/\partial\hat{x}, \quad j_{y7}^{(0,0)} = \partial\phi_7^{(0,0)}/\partial y.$$

The variables  $v_7^{(-1,-1)}$  and  $j_{z7}^{(0,0)}$  are zero while the others are given by

$$h_7^{(1,1)} = h_0 - a^{-\frac{1}{2}}[\frac{1}{3} - \exp(-\xi a^{-\frac{1}{2}})], \quad j_{x7}^{(1,0)} = -a^{-1}\exp(-\xi a^{-\frac{1}{2}}).$$

Half of the  $O(1)$  mass flux flows from the free shear layer into the outer intersection at  $z = -1$ , where it is turned and fed into the downstream outer sublayer. The  $O(M^{-\frac{1}{2}})$  current flux in the negative- $x$  direction inside the outer sublayer passes unchanged through the outer intersection and on into the upstream core at  $x = 0, z = -1$ . The inner intersection 8 is a viscous subregion which satisfies the boundary conditions at the wall and matches the outer intersection as well as the upstream side layer and the downstream inner sublayer. The solution is easily obtained, but is of no particular interest here.

The electrical circuit of the  $O(M^{-\frac{1}{2}})$  current flux is closed through a plane potential current flow in the upstream core. To determine this, we note that  $h_7^{(1,1)}$  varies from  $h_0 + \frac{2}{3}a^{-\frac{1}{2}}$  at  $\xi = 0$  to  $h_0 - \frac{1}{3}a^{-\frac{1}{2}}$  as  $\xi \rightarrow \infty$ . The upstream core sees the variation as a discontinuity in the boundary conditions on (the current function)  $h_4^{(1,1)}$  at  $x = 0, z = -1$ . If now the reference pressure  $h_0$  is chosen so that  $h_4^{(1,1)} = 0$  as  $x \rightarrow -\infty$ , i.e.

$$h_0 = -\frac{2}{3}a^{-\frac{1}{2}},$$

then  $h_4^{(1,1)}$  is a harmonic function of  $x$  and  $z$  which satisfies the boundary conditions

$$h_4^{(1,1)} = 0 \begin{cases} \text{as } x \rightarrow -\infty & \text{for } |z| \leq 1, \\ \text{at } z = \pm 1 & \text{for } -\infty < x \leq 0 \end{cases}$$

and

$$h_4^{(1,1)} = -a^{-\frac{1}{2}} \quad \text{at } x = 0 \quad \text{for } |z| \leq 1.$$

The currents closing the circuit are then given by

$$j_{x6}^{(1,1)} = \partial h_4^{(1,1)}/\partial z, \quad j_{z4}^{(1,1)} = -\partial h_4^{(1,1)}/\partial x.$$

The solution can easily be obtained by conformal mapping, but its precise form is not important.

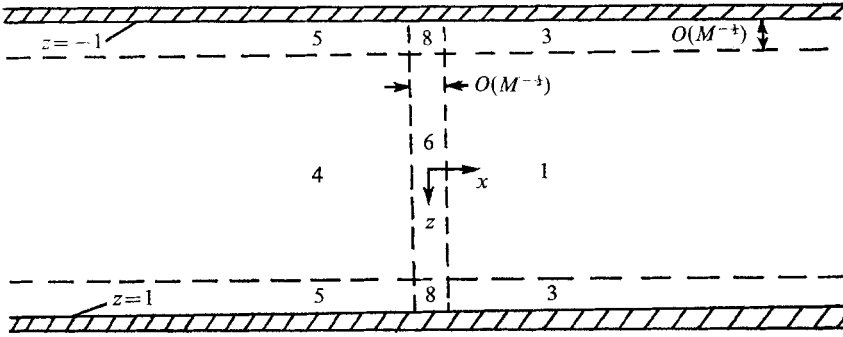


FIGURE 5. *y* section showing subregions for  $b = O(M^{-1/2})$ .

**4. Small slope:  $b = \alpha M^{-1/2}$**

As  $b$  becomes comparable with  $M^{-1/2}$ , the double expansion used in § 3 collapses back into a single-parameter expansion in powers of  $M^{-1/2}$ , but now the coefficient functions are the sums of all terms in each row of the double expansion, just as the coefficients in the single expansion for  $b = O(1)$  were the sums of all terms in each column. Physically, as  $b$  approaches  $\alpha M^{-1/2}$ , the downstream outer sublayers for intermediate slope spread until they meet in the centre of the duct. As they spread these layers carry the  $O(1)$  mass flux and the  $O(M^{-1/2})$  current flux into the downstream core.

The various subregions for this transitional stage (shown in figure 5) are the downstream core 1, downstream side layers 3, upstream core 4, upstream side layers 5, free shear layer 6 and intersections 8. There are no subregions numbered 2 or 7 because the downstream outer sublayers 2 and the outer intersections 7 of § 3 have spread into the core and the free shear layer respectively. Table 1 still applies; note that  $\partial/\partial x = O(M^{-1/2})$  in the diverging portion of the duct ( $x > 0$ ). The  $O(1)$  electric potential and the  $O(M^{-1/2})$  pressure are written as power series in  $M^{-1/2}$ :

$$\phi = \phi^{(0)} + M^{-1/2}\phi^{(1)} + M^{-1}\phi^{(2)} + \dots, \quad h = M^{-1/2}h^{(1)} + M^{-1}h^{(2)} + \dots$$

The transverse velocity  $w_6^{(-1)}$  in the free shear layer is the only  $O(M^{1/2})$  variable in the entire flow.

In the downstream core 1, the substitution  $X = M^{-1/2}x$  compresses the  $x$  co-ordinate so that all derivatives are order one. The core variables which satisfy the governing equations (1) are

$$\begin{aligned} \phi_1^{(0)} &= y\Omega + \Psi, & h_1^{(1)} &= H, & u_1^{(0)} &= -y\partial\Omega/\partial z - \partial\Psi/\partial z, & v_1^{(0)} &= G, \\ v_1^{(1)} &= y\partial^2 H/\partial z^2 + \hat{G}, & w_1^{(1)} &= y\partial\Omega/\partial X + \partial\Psi/\partial X - \partial H/\partial z, \\ j_{x1}^{(1)} &= \partial H/\partial z, & j_{y1}^{(0)} &= \Omega, & j_{y1}^{(1)} &= \hat{\Omega}, & j_{z1}^{(2)} &= \bar{\Omega}, & j_{z1}^{(2)} &= -\partial H/\partial X, \end{aligned}$$

where  $\Omega, \Psi, H, G, \hat{G}, \hat{\Omega}$  and  $\bar{\Omega}$  are integration functions of  $X$  and  $z$ . Applying the Hartmann conditions, which are

$$v_1^{(0)} = v_1^{(1)} \mp \alpha u_1^{(0)} = j_{y1}^{(0)} = j_{y1}^{(1)} = j_{y1}^{(2)} \mp \alpha j_{x1}^{(1)} \pm \partial u_1^{(0)}/\partial z = 0 \quad \text{at } y = \pm(a + \alpha X),$$

we find that  $G$ ,  $\Omega$ ,  $\hat{G}$ ,  $\hat{\Omega}$  and  $\tilde{\Omega}$  are all zero and that  $\Psi$  and  $H$  must satisfy

$$(a + \alpha X) \frac{\partial^2 H}{\partial z^2} + \alpha \frac{\partial \Psi}{\partial z} = \alpha \frac{\partial H}{\partial z} + \frac{\partial^2 \Psi}{\partial z^2} = 0.$$

Since the flow is symmetric in  $z$ ,

$$\Psi = -\mathcal{F} \sinh(\alpha z(a + \alpha X)^{-\frac{1}{2}}), \quad H = \mathcal{D} + \mathcal{F}(a + \alpha X)^{-\frac{1}{2}} \cosh(\alpha z(a + \alpha X)^{-\frac{1}{2}}),$$

where  $\mathcal{F}(X)$  and  $\mathcal{D}(X)$  will be determined by matching the downstream side layers 3.

We need only consider the side layer at  $z = -1$ , where the substitutions  $\zeta = M^{\frac{1}{2}}(z + 1)$  and  $X = M^{-\frac{1}{2}}x$  are introduced in order to stretch the  $z$  co-ordinate and to compress the  $x$  co-ordinate. This layer does not carry any of the  $O(1)$  mass flux or the  $O(M^{-\frac{1}{2}})$  current flux, so that, by virtue of the governing equations (1), several simple results follow immediately, namely,

$$\begin{aligned} \phi_3^{(0)} &= \mathcal{F} \sin[\alpha(a + \alpha X)^{-\frac{1}{2}}], & h_3^{(1)} &= \mathcal{D} + \mathcal{F}(a + \alpha X)^{-\frac{1}{2}} \cosh[\alpha(a + \alpha X)^{-\frac{1}{2}}], \\ h_3^{(2)} &= h_1^{(2)}(X, -1) - \alpha \zeta \mathcal{F}(a + \alpha X)^{-1} \sinh[\alpha(a + \alpha X)^{-\frac{1}{2}}], \\ v_3^{(0)} &= 0, & j_{z3}^{(1)} &= -\alpha \mathcal{F}(a + \alpha X)^{-1} \sinh[\alpha(a + \alpha X)^{-\frac{1}{2}}], \\ w_3^{(1)} &= (a + \alpha X)^{-1} d\{\mathcal{F}(a + \alpha X) \sinh[\alpha(a + \alpha X)^{-\frac{1}{2}}]\}/dX. \end{aligned}$$

However,  $w_3^{(1)}$  must be zero at the wall, so that

$$\mathcal{F} = c/(a + \alpha X) \sinh[\alpha(a + \alpha X)^{-\frac{1}{2}}],$$

where the integration constant  $c$  is determined by the mass flux condition (2):

$$\int_{-1}^1 \int_{-(a + \alpha X)}^{a + \alpha X} u_1^{(0)}(X, y, z) dy dz = 4c,$$

so that  $c = a$ .

The  $O(M^{-\frac{1}{2}})$  electric potential  $\phi_3^{(1)}$  satisfies the equation

$$\partial^2 \phi_3^{(1)}/\partial y^2 = \partial^4 \phi_3^{(1)}/\partial \zeta^4$$

and the boundary conditions

$$\partial \phi_3^{(1)}/\partial y = \pm \partial^2 \phi_3^{(1)}/\partial \zeta^2 \quad \text{at} \quad y = \pm(a + \alpha X),$$

$$\phi_3^{(1)} = \phi_1^{(1)}(X, y, -1) - \alpha a \zeta (a + \alpha X)^{-\frac{3}{2}} \coth[\alpha(a + \alpha X)^{-\frac{1}{2}}] \quad \text{as} \quad \zeta \rightarrow \infty,$$

and

$$\frac{\partial \phi_3^{(1)}}{\partial \zeta} = 0, \quad \frac{\partial^3 \phi_3^{(1)}}{\partial \zeta^3} = -\frac{d\mathcal{D}}{dX} - \frac{d}{dX} \{a(a + X)^{-\frac{3}{2}} \coth[\alpha(a + \alpha X)^{-\frac{1}{2}}]\} \quad \text{at} \quad \zeta = 0.$$

Having determined  $\phi_3^{(1)}$ , the related variables are found to be

$$\begin{aligned} u_3^{(0)} &= -\partial \phi_3^{(1)}/\partial \zeta, & j_{y3}^{(1)} &= \partial \phi_3^{(1)}/\partial y, \\ j_{z3}^{(2)} &= -\frac{\partial^3 \phi_3^{(1)}}{\partial \zeta^3} - \frac{d\mathcal{D}}{dX} - \frac{d}{dX} \{a(a + \alpha X)^{-\frac{3}{2}} \coth[\alpha(a + \alpha X)^{-\frac{1}{2}}]\}. \end{aligned}$$

Integration of the governing equation over the semi-infinite strip

$$|y| \leq a + \alpha X, \quad 0 \leq \zeta < \infty,$$

together with the boundary conditions and the continuity of  $u_3^{(0)}$  at the corners, gives an equation for  $\mathcal{D}(X)$ , namely,

$$\frac{d\mathcal{D}}{dX} = -(a + \alpha X)^{-1} \frac{d}{dX} \{ (a + \alpha X)^{-\frac{1}{2}} \coth [\alpha(a + \alpha X)^{-\frac{1}{2}}] \}.$$

This completes the solution in the downstream core 1 except for an integration constant, the reference pressure  $h_0$ , which will be chosen so that  $h_4^{(1)}$  is zero as  $x \rightarrow -\infty$ .

$\phi_3^{(1)}$  itself can be constructed from heat-source solutions, as before:

$$\begin{aligned} \phi_3^{(1)} = \phi_1^{(1)}(X, y, -1) + \alpha a(a + \alpha X)^{-\frac{1}{2}} \coth [\alpha(a + \alpha X)^{-\frac{1}{2}}] \\ \times [\phi^*(\alpha X, y, \zeta) + \phi^*(\alpha X, -y, \zeta) - \zeta(a + \alpha X)], \end{aligned}$$

where  $\phi^*(X, y, \zeta)$  is the profile function of § 3 and  $\phi_1^{(1)}(X, y, -1)$  is an integration function of  $X$  and  $y$  which plays no significant role in our first-order solution.  $j_{z3}^{(2)}$  is now given by

$$j_{z3}^{(2)} = \alpha a(a + \alpha X)^{-\frac{1}{2}} \coth [\alpha(a + \alpha X)^{-\frac{1}{2}}] - \partial^3 \phi_3^{(1)} / \partial \zeta^3.$$

The flow in the free shear layer is once again determined independently at each  $z$  section, by the jump in  $\phi^{(0)}$  across the layer. Since the  $O(1)$  variables in the upstream core are those for the fully developed solution, the structure of the free shear layer is determined by

$$\phi_6^{(0)} = -z + \frac{1}{4}[4 - \hat{\phi}(\hat{x}, y) - \hat{\phi}(\hat{x}, -y)] [z - \sinh(\alpha z a^{-\frac{1}{2}}) / \sinh(\alpha a^{-\frac{1}{2}})],$$

where the profile function  $\hat{\phi}$  and the co-ordinate  $\hat{x}$  are as defined in § 3. The other non-zero variables are

$$\begin{aligned} w_6^{(0)} = -\partial \phi_6^{(0)} / \partial z, \quad j_{y6}^{(0)} = \partial \phi_6^{(0)} / \partial y, \quad w_6^{(-1)} = \partial \phi_6^{(0)} / \partial \hat{x}, \\ h_6^{(1)} = h_0 + a^{-\frac{1}{2}} \frac{\cosh(\alpha z a^{-\frac{1}{2}})}{\sinh(\alpha a^{-\frac{1}{2}})}, \quad j_{x6}^{(1)} = \alpha a^{-1} \frac{\sinh(\alpha z a^{-\frac{1}{2}})}{\sinh(\alpha a^{-\frac{1}{2}})} - \frac{\partial^3 \phi_6^{(0)}}{\partial \hat{x}^3}. \end{aligned}$$

The  $O(1)$  mass flux passes through the core in both the constant-area portion ( $x < 0$ ) and the diverging portion ( $x > 0$ ), in both of which the flow is constant in the  $y$  direction. The upstream flow is also constant in the  $z$  direction, but the downstream flow varies like  $\cosh(\alpha z a^{-\frac{1}{2}})$ . The  $O(M^{\frac{1}{2}})$  transverse velocity  $w_6^{(-1)}$  in the free shear layer redistributes the mass flux in the  $z$  direction between these two different core flows.

The non-uniform velocity distribution in the diverging portion is linked to the  $O(M^{-\frac{1}{2}})$  current  $j_{x1}^{(1)}$ , which flows in the positive- $x$  direction for  $z > 0$  and in the negative- $x$  direction for  $z < 0$ . Since  $\partial^3 \hat{\phi} / \partial \hat{x}^3$  vanishes as  $\hat{x} \rightarrow \pm\infty$ , there is no jump in  $O(M^{-\frac{1}{2}})$  normal current across the free shear layer and a plane potential current flow in the upstream core is needed to complete the electrical circuit. Choosing a reference pressure

$$h_0 = -a^{-\frac{1}{2}} \coth(\alpha a^{-\frac{1}{2}})$$

makes  $h_4^{(1)}$  a harmonic function of  $x$  and  $z$  satisfying the boundary conditions

$$h_4^{(1)} = 0 \quad \text{at} \quad z = \pm 1 \quad \text{for} \quad -\infty < x \leq 0 \quad \text{or as} \quad x \rightarrow -\infty \quad \text{for} \quad |z| \leq 1$$

and

$$h_4^{(1)} = -\alpha^{-\frac{1}{2}}[\cosh(\alpha\alpha^{-\frac{1}{2}}) - \cosh(\alpha z\alpha^{-\frac{1}{2}})]/\sinh(\alpha\alpha^{-\frac{1}{2}}) \quad \text{at } x = 0 \quad \text{for } |z| \leq 1.$$

The solution for  $h_4^{(1)}$  can easily be obtained by conformal mapping, but its precise form is not important.

As  $\alpha \rightarrow 0$ , the free shear layer disappears,  $h^{(1)}$  vanishes everywhere, the downstream velocity distribution becomes uniform and the fully developed solution is recovered for all  $x$ .

### 5. Extensions and remarks

This analysis can be extended to ducts with diverging or converging side walls at  $z = \pm g(x)$  by following the procedure given in Part 3, with one minor modification for ducts with a small slope (§4). Substituting  $z = z/g(x)$  into the downstream core solution given in §4 gives the corresponding solution for a similar duct with diverging side walls.

The solutions presented in §§3 and 4 can be extended to cover general, slowly varying, fully insulated, rectangular ducts. It is sufficient to consider a duct with walls at  $z = \pm 1$  and at  $y = \pm f(x)$ , where  $|f'| \ll 1$  for all  $x$ . For a portion where  $1 \gg |f'| \gg M^{-\frac{1}{2}}$ , the flow can be divided into a core, outer sublayers and inner sublayers, and the solution in each subregion can be obtained by rescaling the solutions presented in §3 for  $x > 0$ . Locating the origin at the start of such a portion, we compress the  $x$  co-ordinate into

$$X = f(x) - a, \quad a = f(0),$$

so that the slope of the duct with respect to  $X$  is 1. If a double expansion in  $f'(x)$  and  $[f'(x)]^{-1} M^{-\frac{1}{2}}$  is then used, the results in §3 are recovered with  $b = f'(x)$ . Walker (1970) reached the same conclusion by asymptotic analysis of the integro-differential equations governing the side layers in a duct with an arbitrary  $f(x)$  (see Part 3).

In any portion of the duct where  $f'$  is of  $O(M^{-\frac{1}{2}})$  the solution is given by the downstream solution presented in §4. Locating the origin at the start of such a portion, we compress the  $x$  co-ordinate in  $X = M^{-\frac{1}{2}}x$  and expand the solution as a power series in  $M^{-\frac{1}{2}}$  alone. The results of §4 are recovered with the substitutions

$$a \rightarrow f(0), \quad (a + \alpha X) \rightarrow f(x), \quad \alpha \rightarrow M^{\frac{1}{2}}f'(x).$$

The present study was principally concerned with posing the problem correctly; solving it was simple compared with the analysis required in Part 3. The correct subdivision of the flow region and the correct expansions were not obvious at the outset. For example, for an intermediate slope (§3), there might have been an upstream outer sublayer. There might also have been an outer free sublayer at  $x = 0^+$  where  $\partial/\partial x = O(bM^{\frac{1}{2}})$  or an intermediate downstream core (after region 6 and before region 1) with accompanying side layers where  $\partial/\partial x = O(1)$ , in one or the other of which the transverse redistribution of mass flux from the upstream core to the downstream outer sublayer was accomplished without the  $O(M^{\frac{1}{2}})$  velocities in the free shear layer 6. There are similar possibilities

for a small slope (§ 4) which complicated the problem at the outset. Once the correct matched asymptotic expansion scheme is established, the analysis is much more straightforward than that needed in Part 3. The reason is that, for  $b = O(1)$ , the side layer at  $z = -1$  not only must carry the  $O(1)$  mass flux but also must satisfy the no-slip boundary condition at the wall. However, when  $b \ll 1$ , this layer splits into an outer sublayer which carries the flux and an inner sublayer which takes care of the no-slip condition, thus decoupling the two phenomena. Mathematically, the difficulties in Part 3 arise because the boundary conditions at the side wall involve  $\partial/\partial x$ ; but, since  $\partial/\partial x \ll 1$  here, these terms are lost and the analysis is simplified.

We wish to express our deep gratitude to Dr J. C. R. Hunt, who was the first to recognize the need for studies of three-dimensional MHD duct flows. In fact, he has been an active author in the previous papers including Part 3, from which the present work evolved. This research was supported partly by the U.S. Army Research Office, Durham and partly by the National Science Foundation under Grant GP 28483.

#### REFERENCES

- ROBERTS, P. H. 1967 *An Introduction to Magnetohydrodynamics*, pp. 181–190. Elsevier.
- SHERCLIFF, J. A. 1953 Steady motion of conducting fluids in pipes under transverse magnetic fields. *Proc. Camb. Phil. Soc.* **49**, 136–144.
- WALKER, J. S. 1970 Three-dimensional magnetohydrodynamic flow in diverging rectangular ducts under strong transverse magnetic fields. Ph.D. thesis, Cornell University.
- WALKER, J. S., LUDFORD, G. S. S. & HUNT, J. C. R. 1972 Three-dimensional MHD duct flows with strong transverse magnetic fields. Part 3. Variable-area rectangular ducts with insulating walls. *J. Fluid Mech.* **56**, 121–141.